COMPUTATIONAL COMBUSTION 2007, ECCOMAS Thematic Conference
D. Roekaerts, P. Coelho, B.J. Boersma, K. Claramunt (Eds.)
18-20 July 2007, Delft, The Netherlands

DISPLACEMENT SPEEDS IN TURBULENT PREMIXED FLAME SIMULATIONS

M. Day, I. Shepherd, J. Bell, J. Grcar and M. Lijewski

Lawrence Berkeley National Laboratory, Berkeley, California, 94720, USA

Key words: Turbulent premixed flames, displacement speed

Abstract. *The theory of turbulent premixed flames is based on a characterization of the flame as a discontinuous surface propagating through the fluid. The displacement speed, defined as the local speed of the flame front normal to itself, relative to the unburned fluid, provides one characterization of the burning velocity. In this paper, we introduce a geometric approach to computing displacement speed and discuss the efficacy of the displacement speed for characterizing a turbulent flame.*

1 Introduction

For turbulent burning regimes typically encountered in experimental premixed combustion systems, the burning rate of the flame is determined largely by the extent of flame front wrinkling. Wrinkling is initiated by the turbulent field and increases the effective surface area of the flame front. A secondary effect is associated with perturbations to the local flame propagation speed that scale with the local rate of flame area production, or "flame stretch", that results from the strain field directly, or from normal propagation of a curved flame front. A vast body of combustion literature, summarized by Clavin [1], Williams [2] and Law and Sung [3], is devoted to the understanding and parameterizing stretch effects on burning velocity, including its role in stabilizing or exciting the growth of wrinkles in the flame surface. With the increasing ability of computation to simulate real flames, it is interesting to quantify the processes determining flame sensitivity to stretch effects, as well as the response to turbulent strain fields as the source of wrinkling. Applications range from flame control to combustion efficiency and to characterizing emissions.

A surprisingly difficult aspect of studying local flame propagation variability is the definition of the "burning speed" of the flame, in units of length per unit time. Arguably, the most natural physical definition should be tied closely to the rate of fuel mass consumption (or, conversion to combustion products), but there are at least two fundamental problems. Conceptually, the fuel consumption occurs throughout a finite-sized subvolume (the *flame zone*) yet a propagation velocity asserts the presence of a combustion *front*. In this paper, we implement a measure of local consumption speed, S_c, based on the definition in [4, p. 46, eqn. 1], which arbitrarily relates local fuel consumption in the flame zone

to the density of fuel in the reactants. A more problematic issue arises, however, due to the practical difficulties of extracting the fuel destruction rate directly from experimental data.

An alternative definition for flame propagation speed is the "displacement speed" of a contour of a reaction-progress indicator. In the context of a premixed flame, the reaction progress may be associated with a monotonic temperature increase through the flame zone, or the decrease of fuel or oxidizer concentration, and the contour value is typically associated with the location of peak combustion reaction activity. The displacement speed is the speed at which the fuel-air mixture crosses this contour, measured in the frame of the flame, which, of course, requires further definition. Since the scalar properties related to the reaction progress are more directly measurable, the displacement speed has become an acceptable surrogate for the local flame speed in experimental flame studies. Generically, the displacement speed is defined as $S_d = \vec{U}_F \cdot \hat{n} - \vec{U}_G \cdot \hat{n}$, where $\vec{U}_F$ is the local velocity of the flame front in lab coordinates, $\vec{U}_G$ is the gas velocity, and $\hat{n}$ is a unit vector locally aligned with the progress variable gradient and is normal to the flame front. Because the flame induces a volumetric expansion in the flow, $\vec{U}_G$ varies across the finite width of the flame zone. In the conventional definition, $\vec{U}_G$ is evaluated in the cold flow ahead of the flame, so that the definition amounts to using (experimentally measurable) Eulerean quantities to evaluate the flame speed relative to the cold gas.

What are the ramifications of the various definitions of the local flame speed on the interpretation of experimental data used to validate various stretched flame theories? Given a validated numerical simulation of a quasi-steady 3D flame, we may investigate the consequences of various assumptions buried in the definition of S_d, and its relationship to a flame propagation speed that should be relatively insensitive to its precise definition. In this paper, we begin with a time-dependent simulation of a weakly turbulent low-speed laboratory V-flame, and evaluate direct and indirect measures of the local flame propagation speed. We carefully chose the fuel species and mixture fraction to minimize the sensitivity of the local front propagation speed to flow and geometric affects. We develop an approach for verifying this, specifically demonstrating that the computed flame (and indeed the experimental flame it simulates) shows no appreciable spatial variation in local consumption speed, S_c. We then evaluate the local displacement speed by extending to three-dimensions diagnostic methods used to extract S_d from planar experimental data. From these two independent measures of the flame propagation speed, we are in a position to assess the suitability of S_d as a burning velocity surrogate.

2 Background

The concept of a displacement speed has been implicit in models of turbulent flame propagation since Damköhler predicted in 1940 that $v_T = v_L(A_T/A_L) = v_L + v'$ where v is flame velocity, A is flame area, $_L$ and $_T$ indicate laminar and turbulent values, respectively, and v' is the root mean square of velocity fluctuations [5, p. 206]. (In this section of the paper the notation will vary so as to be consistent with each of the several sources.) More

recently this relationship was written $v_T = \bar{v}\,\Sigma$ where $\bar{v}$ is a mean velocity of "flamelets" (small regions of the flame surface) and Σ is the flame surface density [6, p. 1249]. To evaluate the velocity of the flame brush, one also needs Σ which may be given either by algebraic expressions as in the Bray-Moss-Libby model, or by a separate transport equation as in the Coherent Flamelet Model. In these averaged expressions, the turbulent burning velocity refers to the propagation of the flame brush, while the laminar speed and mean velocity are related to the displacement speed of the flame front.

The fuel consumption rate along the flame front has been known to vary since the work of Markstein in 1964. The first order response to changes in local conditions can be parameterized by Markstein numbers for the curvature and strain, or by a single number characterizing flame stretch in terms of flame area generation due to a weighted sum of curvature and flow strain. With the advent of direct numerical simulations of wrinkled flames, and laser diagnostics capable of imaging flow structures and reaction zones, it became possible to either predict or measure changes in local burning speed to investigate the theoretical relationship between this speed and the components of flame stretch. These efforts, however, require a precise definition for the burning speed, and a corresponding procedure for extracting the quantity from experimental diagnostics.

Poinsot, Echekki, and Mungal [4], basing their work on asymptotic analysis of Clavin and Joulin [7], defined the displacement speed as "the normal flame front velocity with respect to the unburned gas," which they formulated as

$$S_d =_{\text{Poinsot et al.}} S^0 \frac{1 - (\mathcal{C}\mathcal{L}/S^0)\nabla_t \cdot v}{1 - (\mathcal{C}\mathcal{L}\kappa)}$$

where S^0 is the laminar burning velocity, $\mathcal{C}$ is a correction parameter of order unity intended to account for possible errors in the asymptotic analysis at high stretch values, $\mathcal{L}$ is a characteristic length scale (the ratio $\mathcal{L}/d$, for a characteristic flame thickness d, is designated a Markstein number in the asymptotic analysis), ∇_t is the divergence tangential to the flame, v is the fluid velocity, and κ is the radius of curvature. Poinsot et al. simulated numerically a quasi-one dimensional model of a two-dimensional Bunsen flame tip; in this very early calculation it was necessary to assume unity Lewis numbers. The investigation of several possible effects on the displacement speed lead to the conclusion that the primary correlation was to stretch. Since this flame is concave to the reactants, it is consistent with later computational work that Poinsot et al. did not report negative displacement speeds.

Najm and Wyckoff [8] in 1997, began from the conceptual definition of Poinsot, Echekki, and Mungal. They expressed the displacement speed of an isocontour of methane mass fraction, $Y_{\mathrm{CH_4}}$, as

$$S_d =_{\text{Najm et al.}} -\frac{\frac{\partial Y_{\mathrm{CH_4}}}{\partial t} + v \cdot \nabla Y_{\mathrm{CH_4}}}{|\nabla Y_{\mathrm{CH_4}}|}$$

where v is the fluid velocity, and $Y_{\mathrm{CH_4}}$ is the mass fraction of methane. Najm and Wyckoff chose the isocontour $Y_{\mathrm{CH_4}} = 0.1$ to define the flame surface in a computational study of

a vortex interacting with a premixed, stoichiometric methane-air flame. They explained changes in displacement speed in terms of changes in flame thickness caused by compressive tangential strain (where the flame broadens) and large tangential stretch (where the flame thins). Negative displacement speeds were observed when the flame is sharply convex to reactants [8, p. 100, fig. 4].

Gran, Echekki, and Chen [9] in 1998 also performed a computational study of a premixed, stoichiometric methane-air flame with the unburned gas preheated to 800 K. They defined the displacement speed as

$$S_d =_{\text{Gran et al.}} -\frac{\nabla(\rho \mathcal{D}_i \nabla Y_i)}{\rho |\nabla Y_i|} - \frac{\omega_i}{\rho |\nabla Y_i|}$$

where ρ is density, and for the i-th species: $\mathcal{D}_i$ is the diffusion coefficient with respect to the mixture, Y_i is the mass fraction, and ω_i is the net rate of production caused by chemical reactions. Gran et al. chose the isocontour $Y_{\text{CH}_4} = 0.02$ as the flame surface. They found a strong correlation between displacement speed and curvature [9, p. 325, fig. 2]. In fact, S_d even becomes negative in regions of positive curvature where the flame is convex to reactants. Gran et al. further decomposed S_d into tangential and normal diffusive components (replacing ∇ in the first term of their formula by $\nabla_t + \nabla_n$, where ∇_n is the divergence in the line normal to the flame surface) plus a reaction component (the final term in their original formula). They found the negative displacement speed in regions of high positive curvature was governed by the tangential diffusion component.

In an experimental study of displacement speed in premixed laminar flames encountering a toroidal vortex ring, Sinibaldi, Mueller, and Driscoll [10] investigated lean methane and propane flames. Particle image velocimetry (PIV) was used to determine the quantities defining the displacement speed which was defined as

$$S_d =_{\text{Sinibaldi et al.}} v_f \cdot n - v_r \cdot n$$

where v_f is the flame velocity vector and v_r the unburned gas velocity ahead of the flame (both in laboratory coordinates), and n is the unit normal to the flame surface oriented toward the reactants. The overall accuracy of the measurements was estimated to be 15 percent. Sinibaldi et al. noted a discrepancy with the earlier computational results of [8] [9] in that no negative displacement speeds were found. They also interpreted their measurements in terms of flame theory and found a significantly greater sensitivity to curvature than suggested by previous reported values for Markstein numbers.

In later experimental work, Sinibaldi et al. [11] studied lean and rich flames augmenting the PIV data by planar laser-induced fluorescence (PLIF)measurements of hydroxyl [OH] to determine the flame boundary. This study reproduced the earlier findings of variable Markstein number larger than previously measured, and reported the first experimental measurement of negative displacement speeds [11, p. 330, fig. 9; p. 333] which were found to correlate with regions of negative strain.

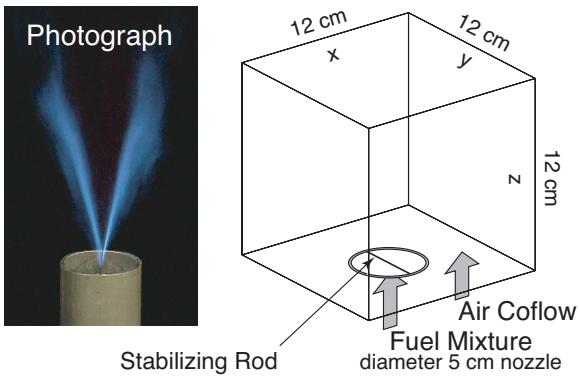

Figure 1: *Photograph of simulated experiment and schematic of numerical simulation domain (photo courtesy of R. Cheng, LBNL).*

3 Simulation methodology

Our analysis is based on a detailed numerical simulation [12] of a steady turbulent V-flame experiment. The simulation provides time-dependent three-dimensional fields for reaction rate progress and fluid velocity. The simulation providing the database for exploration here approximates the experimental V-flame configuration in the LBNL Combustion Laboratory [13]. A schematic of the computational domain, as well as a photograph of the flame experiment, is shown in Figure 3. A methane/air mixture at equivalence ratio $\phi = 0.7$ exits a 5 cm diameter circular nozzle with a mean axial velocity of 3 m/s. The inflowing turbulence is characterized with an integral scale length ℓ_t ∼3.5 mm and a fluctuation intensity of 5.5-7% of the 3 m/s mean inflow speed. The flame is stabilized on a 2 mm wide rod spanning the nozzle. The Markstein number for this fuel mixture is zero [14].

The simulation models only the reacting flow region of the domain; upstream turbulence generation in the nozzle is simulated separately and imposed as a time-dependent boundary condition. A low Mach number model of the reacting Navier-Stokes equations is evolved using an adaptive grid formulation [15]. The fluid is a mixture of perfect gases, and we use a mixture-averaged model for differential species diffusion. We ignore Soret, Dufour and radiative transport processes. The chemical kinetics, transport and thermodynamic properties are evaluated using the DRM-19 subset of the GRI-Mech 1.2 methane mechanism [16] (20 chemical species and 84 fundamental reactions). In particular, there is no explicit model for the speed of combustion propagation, and the thermal zone ahead of the flame has a finite extent captured in detail by the simulation.

The computational domain is a cube, 12 cm on a side, with the nozzle exit centered on the lower face. The simulation is initialized with a small flame just above the rod (approximated simply as a no-flow zone on the inflow face), and as the flow evolves, a flame surface propagates into a statistically stationary V-shape downstream. The domain

is uniformly tiled with a 96^3 grid. Adaptive mesh refinement dynamically focuses blocks of successively finer grid cells in regions of high vorticity and chemical reactivity. The finest cells, $\Delta x = 156.25$ μm, track the flame surface, marked by the presence of the flame radical HCO, and occupy approximately 9% of the 1728 cm^3 domain. The resulting mean and fluctuating scalar fields and velocity fields were consistent with experimental diagnostics, as discussed extensively in [12]. For the present study the simulation was continued for an additional 4.1 ms to provide time-dependent statistics over approximately 1/4 of an integral eddy turnover period.

4 Computation of displacement speed

The local displacment speed of flame propagation normal to itself is computed from snapshots of the 3D time-dependent simulation. This, in effect, represents an extension to three dimensions of the technique utilized by Sinibaldi, et al [11] to process experimental PIV/PLIF measurement data collected on a 2D plane. The basic idea is to examine directly the motion of the flame front relative to the velocity on the unburned side of the flame. For the turbulent V-flame considered here, the mean flow speed is substantially larger than S_d and so the snapshots must be sufficiently separated in time to obtain an acceptable signal-to-noise ratio (here, "noise" is due primarily to interpolation errors associated with sampling the computed solution at arbitrary spatial locations). By trial and error, we arrived at snapshot intervals of approximately $\Delta t = 0.4$ ms, corresponding to 5 coarse-grid time steps of the adaptive low-Mach number integration algorithm. The snapshot data included the three components of velocity and the temperature.

To evaluate the displacement speed we define a reaction progress variable from the temperature field, and assume the $T_f = 1200$K isotherm to be the location the "local flame surface". At this location methane destruction rate is a maximum in a flat, unstrained steady premixed methane flame at $\phi = 0.7$. We confine our analysis to a 4x12x12 cm region centered on the central portion of the stabilization rod; moreover, we exclude the bottom 5 mm (near the rod) and top 2 cm (at the outflow) in order to minimize the impact of the numerical boundary conditions. We exclude the regions extending beyond the ends of the rod, where the flame extinguishes due to lack of fuel. The gas in this region is heated by conduction from the hot products inside the V-shaped region. By focusing on the central region, we avoid processing areas where our reaction progress indicator would incorrectly identify combustion reaction zones. We associate the $T_c = 350$ K isotherm as the cold boundary of the thermal zone ahead of the flame surface. In the laminar flame case, the distance between the T_f and T_c isotherms is approximately 0.6 mm — we will use this as the operational definition of a thermal flame thickness, δ_T.

Because the flow advects ~ 1.2 mm downstream between snapshots, we compute S_d in the following way. Given a point $\vec{x}_F(t_1)$ on the flame at a time t_1, we trace towards the unburned fuel down the integral curves of reaction progress (see Figure 2). The resulting curved 3D path is everywhere normal to the local isotherms at time t_1. On this path there is a (unique) location, $\vec{x}_c(t_1)$, where the temperature is that of the cold boundary,

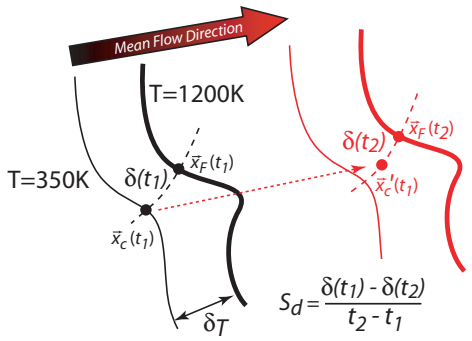

Figure 2: *Computing displacement speed, S_d, from isotherms using discrete snapshots of the solution field. Here, $\delta(t_1)$ is the distance along the flame normal between the two points, $\vec{x}_c(t_1)$ and $\vec{x}_F(t_1)$. $\delta(t_2)$ is the distance along the flame normal at t_2 between the two points, $\vec{x}_c\,'(t_1)$ and $\vec{x}_F(t_2)$. Note that $\vec{x}_c\,'(t_1)$ is NOT on the T_c isotherm; the fluid is heated as it advects from t_1 to t_2.*

$T = T_c$. This location is then numerically advected with the local cold flow velocity over Δt to the time, $t_2 = t_1 + \Delta t$, of the next snapshot of simulation data. The new location, $\vec{x}_c\,'(t_1)$ then seeds the generation of a final integral curve back toward the flame surface at $\vec{x}_F(t_2)$ using solution data at time t_2. Note that the temperature at $\vec{x}_c\,'(t_1)$ is no longer T_c, but has been diffusively heated by the approaching flame. If we compute distance, δ, along the integral curves, $\delta(\vec{x}_2, \vec{x}_1) = \int_{\vec{x}_1}^{\vec{x}_2} ds$ then the rate of flame propagation along the normal, $\hat{n}$, from these sample locations is

$$S_d \approx \frac{\delta(\vec{x}_F(t_1), \vec{x}_c(t_1)) - \delta(\vec{x}_F(t_2), \vec{x}_c\,'(t_1))}{\Delta t}$$

5 Results

Statistics of S_d normalized by the unstrained laminar flame velocity, plotted in Figure 3, indicate a broad distribution that exhibits considerable variation including, consistent with several other studies based on both experimental and computational databases [8, 9, 11]. Examining the data in more detail shows that outliers in the distribution show even larger variability, with displacements speeds as large as 20 times the laminar burning speed. A small but significant fraction of the flame also exhibits negative values for S_d.

Although not derivable from experimental data, a local consumption-based flame speed, S_c, provides an alternative to displacement speed for assessing local flame dynamics, as discussed in the introduction. The methodology for computing S_c from the simulation data is a generalization to three dimensions of the procedure discussed in Bell et al [17]. The normals to the flame isotherm at $t = t_1$ that were used to define the displacement speed are used here to sample the local rate of fuel consumption based on trilinear interpolation. Volumes, Ω (see Figure 4), are constructed to intersect the flame isotherm

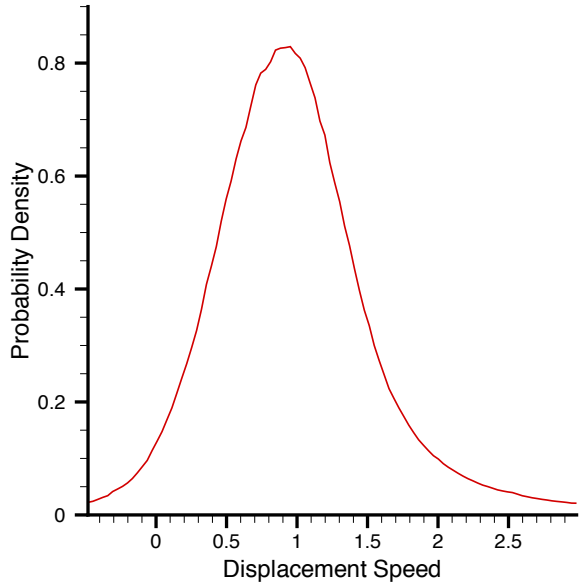

Figure 3: *Representative PDF of displacement speed.*

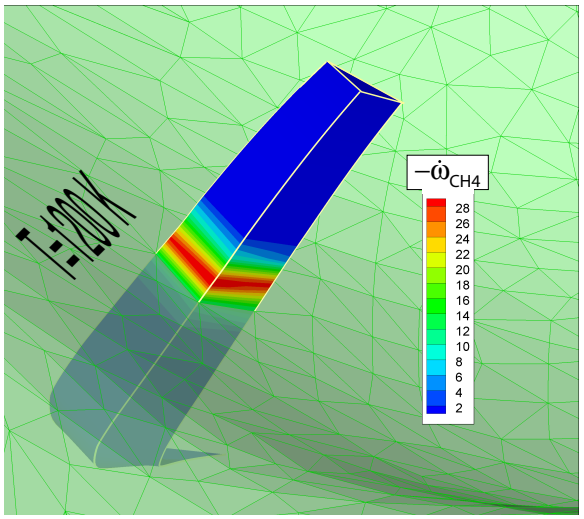

Figure 4: *Construction of wedge volumes, Ω surrounding the $T = T_f$ isotherm, used to define the local fuel consumption speed, S_c. The wedge volume surface is normal the the flame isotherm and is colored with the local value of fuel consumption rate, $-\dot{\omega}_{CH4}$. The intersection of the wedge volume with the isotherm is a triangle of area, A_{Tf}.*

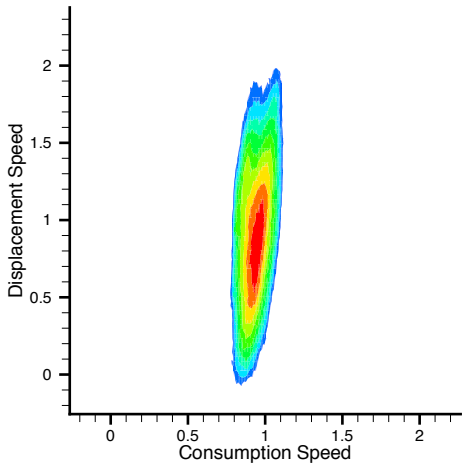

Figure 5: *JPDF of local consumption-based flame velocity vs. displacement speed. (Color scale on JPDF's are are based on the logarithm of the probability.)*

normally, and extend to a distance far enough from the flame isotherm that the fuel destruction rate $-\dot{\omega}_{\mathrm{CH4}}$ vanishes. The local consumption speed, normalized by the burning speed of the corresponding flat laminar flame, S_L, is then defined as

$$S_c = \frac{\int_\Omega -\dot{\omega}_{\mathrm{CH4}}}{A_{Tf} s_L (\rho Y_{\mathrm{CH4}})_{\mathrm{inlet}}}$$

where $(\rho Y_{\mathrm{CH4}})_{\mathrm{inlet}}$ is the density of fuel in the inlet stream, and A_{Tf} is the area of intersection of the volume Ω with the flame isotherm. Note that this definition is sensitive to the particular isotherm used to define the flame, but only the extent that A_{Tf} varies with T_f over Ω. This variation is, however, negligible over 99% of the flame surface throughout the range 1000K to 1500K, meaning that the definition of S_c given above is essentially independent of T_f. In Figure 5 we show a joint PDF of S_d and S_c. The figure shows very little variation in the consumption speed over the entire flame surface, consistent with near zero Markstein number for methane-air flames at $\phi = 0.7$ ([14]), and underscores that the variations in displacement speed appear to be unrelated to variation in local fuel consumption.

Flame theory suggests that S_d should correlate with flame stretch, which combines the effects of curvature and strain. In Figure 6 we show the joint PDF of S_d and the mean flame curvature, taken on the $T = T_f$ surface. Here, negative curvature is when the center of curvature is on the reactants side of the flame surface. In general, the curvature of a 2D surface in 3-space is given by two principal curvatures, κ_1, κ_2. The mean curvature, $\kappa = \kappa_1 + \kappa_2$ is relatively large, either when only one is large (a ridge in the surface) or in bowl-shaped regions where κ_1 and κ_2 have the same sign. We see a strong negative correlation between displacement speed and curvature. Along the normal

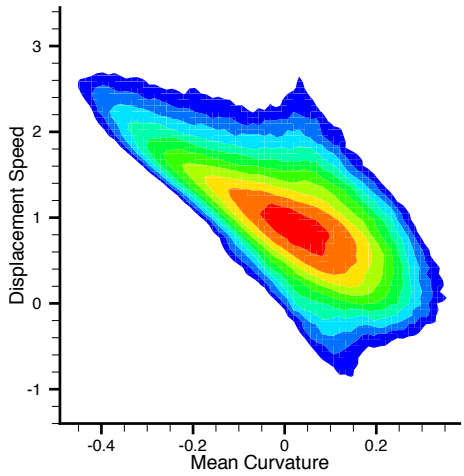

Figure 6: *JPDF of mean curvature of the flame surface vs. displacement speed.*

to the local flame progress variable the flame appears to move more quickly in regions high negative curvature. However, it is likely that the diagnostic is strongly impacted by Huygen's-type propagation effects (normal propagation of a curved surface), which tend to shorten cusps in the surface that point toward the products. A better measure of surface propagation speed would use a distance function that is based on the solution of the Eikonal equation, as discussed in [18]. It is worth noting that such a construction is not presently possible based on a two-dimensional characterization of the flame surface, as obtained, for example, from experimental Mie scattering images. In future work, we will attempt to address whether the correlation of S_d with curvature for this case is entirely due to the Huygen's propagation effect.

Assessing the relationship between S_d and the flow strain rate is more problematic. Theoretical analyses and scaling parameterizations, such as those used to construct the regime diagrams discussed in [19, 20], are based on the cold flow turbulence *approaching* the flame prior to the dilation effects due to heat release within the flame front. Conventionally, the strain field is therefore evaluated in the cold region upstream of the preheat zone. Note that there is a large literature on the generalization of classical flame theory to "thick" flames, see [21–24] and references therein. The theory suggests that we should expect the displacement speeds to be correlated to the strain evaluated upstream (along the normals constructed above) where $T = T_c$. A more straightforward approach, which is not consistent with theory, is to simply evaluate the tangential strain rate at the flame surface ($T = T_f$). In Figure 7a,b we show JPDF's of S_d using both of these definitions of tangential strain. In Figure 7c we show a JPDF of strain rate at the flame and mean curvature, indicating that the strain rate at the flame is strongly correlated to curvature. Thus, the variation in S_d along the flame appears to be explained primarily by the cor-

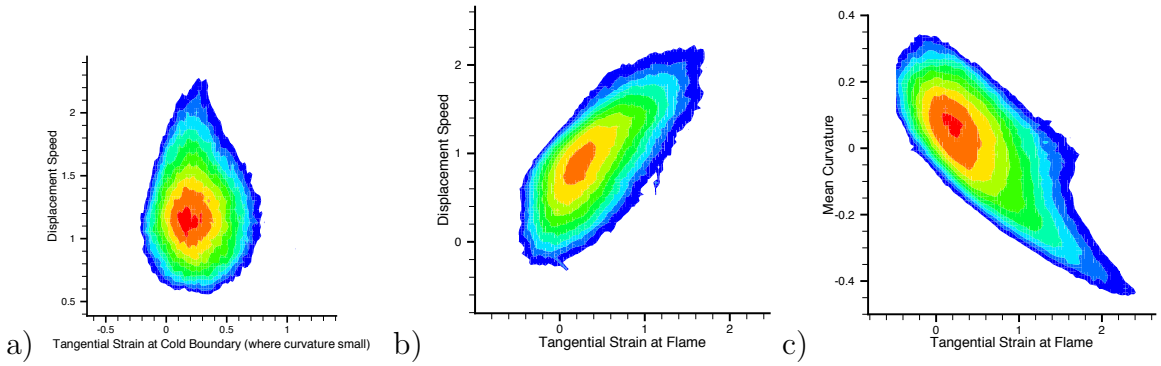

Figure 7: *a) JPDF of cold tangential strain and displacement speed. b) JPDF of tangential strain in the flame surface and displacement speed. c) JPDF of tangential strain in the flame surface and mean curvature*

relation of S_d with curvature, strain effects only contributing a minor effect. A similar observation was made by Haworth and Poinsot [25]. Bell at al. [17] also reach a similar conclusion considering local consumption speed, S_c, instead of displacement speed for flames with nontrivial Markstein effects. Pope [26] discusses in more detail the interrelationship of curvature and strain. The difficulties with defining a local strain rate for the definition of stretch suggests that an integral-based approach, as for example [24, 27], is needed to obtain a more robust and physically meaningful method for computing stretch. Future work here will include exploring integral measures based on the wedge volumes, Ω, defined above, and the flux of material across the wedge volume boundary over the entire flame zone.

A relatively direct measure of the integrated effects of strain on S_d is given by measuring the rate of change in flame thickness. Here we define the flame thickness to be the distance from the $T = T_c$ contour to the $T = T_f$ contour. Alternative measures of flame thickness include quantities such as a scaled inverse maximum temperature gradient. Our definition, while not standard, has the property of focusing on disruptions in the thermal profile in regions away from the primary combustion zone, and is more closely linked to the algorithm specified above for computing S_d.

In Figure 8 we show a scatter plot of S_d versus the rate of change in flame thickness, with both axes normalized by the laminar burning velocity. The data, particularly the outliers with large positive and negative values of S_d, show a strong correlation, suggesting that strain effects within the flame zone are at least partially responsible for the some of the observed large variations in S_d. However, it appears that it is the *integrated* strain field as the cold fluid parcels traverse the preheat zone that affects the displacement speed, rather than the instantaneous strain rate at any point along the path.

A final observation about the structure of this flame is shown in Figure 9, which depicts a joint PDF of flame thickness and the angle of the flame with respect to vertical axis. This diagnostic shows a correlation that implies that flame elements with upward pointing

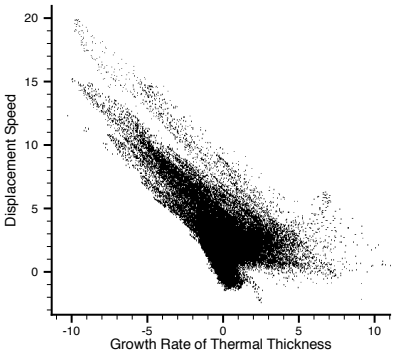

Figure 8: *Scatter plot of S_d and rate of change of flame thickness.*

normals are typically thicker than flame elements that are oriented downward. Additional data (not shown) shows that this angle is not correlated to either curvature or strain, hence the correlation does not represent any simple auxiliary correlation between flame structure and orientation. Estimates suggest that the time scales are not long enough for gravitational acceleration to account for this effect; instead, it must be related to the orientation of the flame with respect to the mean flow.

6 Conclusions

Although commonly accepted as a consequence of the definition of S_d (and affected by processes such as localized flame thickening), the broad range of values observed for the displacement speed does not appear to be consistent with local measures of the burning rate of the flame. Negative values of S_d, as well as unphysically large positive values have been obtained in this and a number of earlier studies. In the simulation data studied here, a turbulent inflow of premixed fuel produces regions of large strain and curvature at the cold boundary of the flame. We might expect such conditions to lead to local variations in S_d, but the phenomenology of the variations we actually observe suggest a more significant breakdown of the theoretical constructs. We find evidence that the diagnostic is strongly skewed by multi-dimensional, time-dependent flow straining in a way that cannot easily be deconvolved without a full characterization of the velocity and scalar fields. To the extent possible, we have isolated these effects by working in a regime without observed Markstein effects, while basing the analysis on a realizable quasi-steady turbulent system. The diagnostics relied on the three-dimensional, time-dependent fields for the velocity fields and the scalar measure of reaction progress, and are therefore available only through detailed simulations; volumetric time-dependent experimental diagnostics are not currently available for flames in this regime.

Future studies in this area will focus on more a complete characterization of the in-

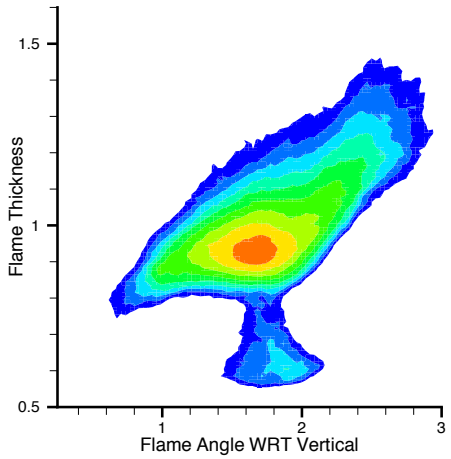

Figure 9: *PDF of local flame surface angle with respect to vertical vs. flame thickness.*

tegrated strain effects through the preheat zone, and on improved measures of three-dimensional front propagation (such as computing a proper three-dimensional distance by solving the Eikonal equation). Also, it will be interesting to understand the impact of our observations on the processing of experimental data based on planar data collection techniques. Clearly, mean curvature effects, flow strain and flame thickness measurements are skewed in this circumstance by the projection of the flame surface onto the plane of data collection. Typical arguments to correct for this phenomena must assume a distribution of orientation angle. This distribution will depend strongly on the experimental configuration and turbulence regime interest. However, with detailed simulation data at the appropriate temporal and spatial scales, we are in the position to evaluate the assumptions implicit in 2D experimental diagnostics.

REFERENCES

[1] Clavin, P., *Proc. Combust. Inst.*, 28:569 (2000).

[2] Williams, F. A., *Prog. Energy Combust. Sci.*, 26:65 (2000).

[3] Law, C. K. and Sung, C. J., *Prog. Energy Combust. Sci.*, 26:459–505 (2000).

[4] Poinsot, T., Echekki, T., and Mungal, M. G., *Combustion Science and Technology*, 81:45–73 (1992).

[5] Warnatz, J., Maas, U., and Dibble, R. W., *Combustion* (3rd ed), Springer-Verlag, Berlin, 2001.

[6] Veynante, D., Duclos, J. M., and Piana, J., *Proc. Combust. Inst.*, 25:1249–1256 (1994).

[7] Clavin, P. and Joulin, G., *J. Physique–Lettres*, 44:L1–L12 (1983).

[8] Najm, H. N. and Wyckoff, P. S., *Combust. Flame*, 110(1–2):92–112 (1997).

[9] Gran, I. R., Echekki, T., and Chen, J. H., *Proc. Combust. Inst.*, 27:323–329 (1998).

[10] Sinibaldi, J. O., Mueller, C. J., and Driscoll, J. F., *Proc. Combust. Inst.*, 27:827–832 (1998).

[11] Sinibaldi, J. O., Driscoll, J. F., Mueller, C. J., Donbar, J. M., and Carter, C. D., *Combust. Flame*, 133(3):323–334 (2003).

[12] Bell, J. B., Day, M. S., Shepherd, I. G., Johnson, M., Cheng, R. K., Grcar, J. F., Beckner, V. E., and Lijewski, M. J., *Proc. Natl. Acad. Sci. USA*, 102(29):10006–10011 (2005).

[13] Bedat, B. and Cheng, R. K., *Combust. flame*, 100:485–494 (1995).

[14] Tseng, L.-K., Ismail, M. A., and Faeth, G. M., *Combust. Flame*, 95:410–425 (1993).

[15] Day, M. S. and Bell, J. B., *Combust. Theory Modelling*, 4:535–556 (2000).

[16] Frenklach, M., Wang, H., Goldenberg, M., Smith, G. P., Golden, D. M., Bowman, C. T., Hanson, R. K., Gardiner, W. C., and Lissianski, V., "GRI-Mech—an optimized detailed chemical reaction mechanism for methane combustion," Gas Research Institute Technical Report No. GRI-95/0058, `http://www.me.berkeley.edu/gri_mech/`.

[17] Bell, J. B., Day, M. S., Grcar, J. F., and Lijewski, M. J., *Comm. App. Math. Comput. Sci.*, 1(1):29–51, November (2005), Also appears as LBNL Report LBNL-58751.

[18] Sankaran, R., Hawkes, E. R., Yoo, C. Y., Chen, J. H., Lu, T., and Law, C. K., *Proceedings of the 5$^{\text{th}}$ US Combustion Meeting (CD-ROM)*, , March (2007), Paper B09.

[19] Peters, N., *Turbulent Combustion* , Cambridge University Press, Cambridge, 2000.

[20] Borghi1984, (Bruno, C. and Casci, C., editors), *Recent Advances in Aeronautical Science*, Pergamon, 1984.

[21] Chung, S. H. and Law, C. K., *Combust. Flame*, 72:325–336 (1988).

[22] Goey, L. P. H. de and Thije Boonkkamp, J. H. M. ten, *Combustion Science and Technology*, 122:399–405 (1997).

[23] Goey, L. P. H. de, Mallens, R. M. M., and Thije Boonkkamp, J. H. M. ten, *Combust. Flame*, 110:54–66 (1997).

[24] Goey, L. P. H. de and Thije Boonkkamp, J. H. M. ten, *Combust. Flame*, 119:253–271 (1999).

[25] Haworth, D. C. and Poinsot, T. J., *J. Fluid Mech.*, 244:405–436 (1992).

[26] Pope, S. B., *Int. J. Engng. Sci.*, 26:445–469 (1988).

[27] Oijen, J. A. van, Groot, G. R. A., Bastiaans, R. J. M., and Goey, L. P. H. de, *Proc. Combust. Inst.*, 30(1):657–664 (2005).